Biomedicine & Pharmacotherapy 100 (2018) 324–334

Contents lists available at ScienceDirect

Biomedicine & Pharmacotherapy

journal homepage: www.elsevier.com/locate/biopha

Evaluation of the anti-hypertensive effect of Tengfu Jiangya tablet by combination of UPLC-Q-exactive-MS-based metabolomics and iTRAQ-based proteomics technology

Yanpeng Tian[a,b], Feng Jiang[b], Yunlun Li[a,b,*], Haiqiang Jiang[c,**], Yanjun Chu[a,b], Lijuan Zhu[d], Weixing Guo[e]

[a] First Clinical Medical College, Shandong University of Traditional Chinese Medicine, Jinan 250355, Shandong, China
[b] Department of Cardiology, Affiliated Hospital of Shandong University of Traditional Chinese Medicine, Jinan 250011, Shandong, China
[c] Central Laboratory, Shandong University of Traditional Chinese Medicine, Jinan 250355, Shandong, China
[d] Department of Traditional Chinese Medicine, Liaocheng Hospital of Traditional Chinese Medicine, Liaocheng 252000, Shandong,China
[e] Office of the Director, Shandong Academy of Medical Sciences, Jinan 250062, Shandong, China

ARTICLE INFO

Keywords:
Tengfu Jiangya tablet
Metabolomics
Proteomics
Hypertension
iTRAQ

ABSTRACT

Objective: Tengfu Jiangya tablet (TJT) is a traditional Chinese medicine formulation composed of *Uncaria rhynchophylla* and *Semen raphani*. It is a hospital preparation that is widely used in clinics for treating hypertension. A previous metabolomics study reported that TJT exerted a protective effect on hypertension by restoring impaired NO production, ameliorating the inflammatory state, and vascular remodeling. A clinical proteomics study also revealed five key target proteins during TJT intervention. This study aimed to integrate proteome and metabolome data sets for a holistic view of the molecular mechanisms of TJT in treating hypertension.

Methods: Serum samples from spontaneously hypertensive rats and Wistar Kyoto rats were analyzed using ultra-high performance liquid chromatography coupled to Q Exactive hybrid quadrupole-Orbitrap mass spectrometry (UPLC-Q-Exactive-MS)-based metabolomics technology and isobaric tags for relative and absolute quantitation (iTRAQ)-based quantitative proteomics technology. Moreover, we selected two candidate proteins and determined their expression levels in rat serum using an enzyme-linked immunosorbent assay (ELISA).

Results: A total of 20 potential biomarkers and 14 differential proteins in rat serum were identified. These substances were mainly involved in three biological pathways: the kallikrein–kinin pathway, the lipid metabolism pathway, and the PPARγ signaling pathway.

Conclusions: The results suggested that TJT could effectively treat hypertension, partially by regulating the above three metabolic pathways. The combination of proteomics and metabolomics provided a feasible method to uncover the underlying interventional effect and therapeutic mechanism of TJT on spontaneously hypertensive rats.

1. Introduction

Omics techniques with advanced analysis tools, such as liquid and gas chromatography and mass spectrometry, have been well utilized in medical diagnostics and basic research. They have greater probability of revealing new therapeutic targets than traditional methods [1,2]. Based on a single set of data, a number of new disease-related factors have been identified in the process of disease research. Metabolomics is mainly applied in discovering biomarkers and their perturbed pathways. It can monitor the pathological changes in the body, intervene early in the disease and reveal the therapeutic mechanisms. With a range of different analytical platforms and multivariate statistics methods, metabolomics is extensively utilized to discover the potential biomarkers in diseases. Isobaric tags for relative and absolute quantitation (iTRAQ) is a valid method for identifying the level of differentially expressed proteins (DEPs). Proteomics technologies are mainly used to identify thousands of de-regulated dynamic proteins and their interactions in a cell or body fluid, while metabolomics methods are used to analyze the level changes of low molecular weight compounds in a cell and extracellular fluids [2,3]. In recent years, omics techniques

* Corresponding author at: Affiliated Hospital of Shandong University of Traditional Chinese Medicine, Wenhua Xi Road, Jinan 250011, Shandong, China.
** Corresponding author at: Center Laboratory of Shandong University of Traditional Chinese Medicine, Daxue Road, Jinan 250355, Shandong, China.
E-mail addresses: yunlun.lee@hotmail.com (Y. Li), jhq12723@163.com (H. Jiang).

https://doi.org/10.1016/j.biopha.2018.02.025
Received 17 November 2017; Received in revised form 7 February 2018; Accepted 9 February 2018

have been more frequently used in exploring potential biomarkers and therapeutic targets of hypertension [4].

Hypertension is a global public health challenge caused by a combination of factors, with or without a variety of cardiovascular risk factors. The mechanism of hypertension is quite complex. It is not only the most common chronic disease worldwide, but also a major risk factor of cardiovascular disease and stroke [5–7]. It currently affects more than 1 billion individuals in both developed and developing countries. According to estimates, about 4.5% of the global disease burden is caused by hypertension [8,9]. Its prevalence will increase by 50% from 1 to 1.5 billion adults by 2020, according to the World Health Organization (WHO) report [10]. About seven million deaths are related to hypertension and its cardiovascular complications annually [11]. Many animal models have been used to study hypertension, including spontaneously hypertensive rat (SHR), stroke-prone SHR (SHRSP), New Zealand hereditary hypertensive rats (GH), Dahl salt-sensitive hypertensive rats (DS) and the like. Among them, SHR is the most widely used animal model that has been internationally acknowledged to be closest to essential hypertension. It is similar to human hypertension in many ways, including in terms of its pathogenesis, cardiovascular complications, peripheral vascular resistance changes and salt sensitivity. Wistar Kyoto (WKY) rat is the normal blood pressure control group of SHR and both modes were developed from Wistar rats. In treatment, various anti-hypertensive drugs, like diuretics, beta-blockers, calcium-channel blockers, and angiotensin-converting enzyme inhibitors, have been used to reduce mortality. Their therapeutic effects, however, are not satisfactory, with a variety of side effects, such as tachycardia and gastro-intestinal upset.

Traditional Chinese medicine (TCM) has been extensively used in China and Eastern Asia for the treatment of hypertension for thousands of years. TCM has been increasingly accepted by the world in recent years and has been widely used clinically. Tengfu Jiangya tablet (TJT) is a TCM formula composed of *Uncaria rhynchophylla* and *Semen raphani*. Our preliminary metabolomics study, based on a high performance liquid chromatography/mass spectrometry (HPLC-TOF-MS) method, has found that TJT exerted its anti-hypertensive effect mainly by improving NO production, amelioration of inflammatory state and vascular remodeling [12]. Also, a clinical serum proteomic study with quantitative proteomic techniques was performed to explore its effects and mechanism on essential hypertension, and 5 target biomarkers were discovered closely related to vascular endothelial injury, which is a key factor of the occurrence and development of hypertension [13]. However, the dysfunctions of both proteins and metabolites play an important role in the pathological process of hypertension. The combination of proteome and metabolome profiling can provide new insights into the understanding of biological systems. Moreover, the level of proteins can influence the metabolic profile, while the concentration of metabolites can affect protein expression [1], and the integrative pathway analysis of both proteins and metabolites will thus help to interpret the underlying biological phenomena. Therefore, in this work, an ultra-high performance liquid chromatography coupled with a Q Exactive hybrid quadrupole-Orbitrap mass (UPLC-Q-Exactive-MS)-based metabolomics technique was applied to discover biomarkers in rat serum, and their perturbed pathways and changes after TJT intervention at higher resolution than TOF that was used in our previous study. Meanwhile an iTRAQ-based proteomics technique was utilized for searching for the differential proteins expressed in the bio-samples and observing their variations after intervention with TJT. Finally, we integrated the data from both analyses to elucidate the TJT effects in protecting against hypertension.

2. Materials and methods

2.1. Materials and reagents

HPLC-grade acetonitrile and methanol were purchased from Merck KGaA (Darmstadt, Germany); formic acid was obtained from TEDIA Company Inc. (Fairfield, USA); ultrapure water was prepared using a Milli-Q water purification system (Millipore Corporation, MA, USA); leucine enkephalin was purchased from Sigma-Aldrich (St. Louis, MO, USA). All other reagents were of HPLC grade. The assay kits for myeloperoxidase (MPO) and kininogen 1 (KNG1) were purchased from Uscn Life Science Inc. (Wuhan, China). TJTs were purchased from the Affiliated Hospital of Shandong University of Traditional Chinese Medicine (Jinan, Shandong). The rhynchophylline content was between 1.182 mg and 1.444 mg per tablet and the sinapine thiocyanate content was between 6.001 mg and 7.335 mg per tablet. Before use, TJTs were dissolved in saline to concentrations of 2.50 mg/ml total *Uncaria* alkaloids in suspension and 3.00 mg/ml *Semen raphani* alkaloids in solution, and then stored at 4 °C until use.

2.2. Animal handling

A total of 20 male SHRs and ten male WKY rats weighing 200–220 g were supplied by Vital River Laboratory Animal Technology Co. Ltd. (Beijing, China). All the SHRs were randomly divided into two groups with ten rats in each group: the model group and the TJT-treated group. The WKY rats served as the normal control group. All animals were housed in an air-conditioned room at a temperature of 22 ± 2 °C, 55 ± 5% humidity, and a 12 h dark/light cycle. They were fed with a certified standard diet and tap water *ad libitum*. In the TJT-treated group, 100 mg TJT/200 g body weight was administered intragastrically once a day for 4 weeks and control groups were given equal quantities of physiological saline. The blood pressure of each rat was measured three times in a row on the tail artery by a noninvasive method pre-administration and then 1, 2, 3, and 4 weeks post administration. All experimental procedures were approved by the Animal Care and Ethics Committee of Shandong University of Traditional Chinese Medicine. Special care was taken to minimize animal suffering.

2.3. Sample collection and preparation

Serum samples (100 µl) were collected from the animals for metabolic profiling experiments. Methanol (300 µl) was added to each serum sample and the samples were then vortexed for 1 min to precipitate the proteins. The samples were then centrifuged at 13,000 rpm for 15 min and transferred to vials for UPLC-MS analysis. A quality control (QC) sample was prepared by mixing an equal aliquot (40 µl) from all serum samples for the optimization of the UPLC-MS conditions, and the method validation.

2.4. Metabolic profiling platform

2.4.1. Chromatography and mass spectrometry conditions

Metabolic profiling analysis was performed using an UPLC-Q-Exactive-MS system. Chromatographic analysis was performed using an UltiMate 3000 UPLC system (UPLC, Thermo Scientific). A 2-µl aliquot of the prepared sample solution was injected onto a Thermo C18 column (Hypersil GOLD aQ, 100 × 2.1 mm, 1.9 µm). The column temperature was set at 45 °C and the flow rate was 0.3 ml/min. The mobile phase consisted of a linear gradient system of (A) 0.1% formic acid in water and (B) 0.1% formic acid in acetonitrile: 0–1.0 min: 0–2% B; 1.0–3.0 min: 2–40% B; 3.0–15.0 min: 40–98% B. Mass spectrometry detection was performed using a Q Exactive™ hybrid quadrupole-Orbitrap mass spectrometer in both positive and negative ionization modes. The optimal analysis conditions were set as follows: ion source: heated electrospray ionization probe; source temperature: 350 °C; capillary temperature: 300 °C; sheath gas: 45 arb; auxiliary gas: 10 arb; mass collecting range: *m/z* 80–800; resolution: 70,000; and (S)-lens RF level: 55. The above parameters were the same in both modes. The capillary voltage was set at 3.5 kV in positive mode and 3.0 kV in negative mode. Further MS/MS analysis was done on potential biomarker

ions and the collision energy was automatically optimized.

2.4.2. Data processing

Raw data were converted into mzXML format by ProteoWizard and processed with XCMS (http://metlin.scripps.edu/download/) for peak recognition, alignment, and correction. The parameters used were default settings except for the following: ppm = 10, bw = 10, and snthresh = 20. A visual data matrix containing retention time, *m/z* pairs, sample names, and normalized ion intensities was generated and exported to SIMCA-P 11.5 software (Umetrics AB, Umea, Sweden) for multivariate data analysis.

2.4.3. Data analysis and biomarker identification

The multivariate data matrix was analyzed by SIMCA-P 11.5 software for principle component analysis (PCA) and partial least squares discriminant analysis (PL(S)-DA). In the PC scores plot, each point represents an individual sample and in the PC loadings plot each point represents one mass/retention time pair. Thus, the latter gives an indication of the metabolites that most strongly influence the patterns in the former. From the PCA and PL(S)-DA loading plots, various metabolites could be identified. Variable importance for projection (VIP) values produced in PL(S)-DA were applied to find potential biomarkers and variables with VIP > 1 were further processed by Mass Profiler Professional (Agilent Technologies, USA) for Student's t-test and fold change (FC). Variables with VIP > 1, $p < 0.05$, and FC > 2 were considered to be potential biomarkers. Identification was carried out by searching HMDB (http://www.hmdb.ca/), METLIN (https://metlin.scripps.edu) and KEGG (http://www.genome.jp/kegg/) databases and pathway analysis was performed with the MetaboAnalyst tool (http://www.metaboanalyst.ca).

2.5. iTRAQ-based proteomics analysis

2.5.1. Sample preparation and protein extraction

Plasma was fractionated with a ProteinMiner Protein Enrichment Small-Capacity kit (ProteinMiner; Bio-Rad Laboratories, Hercules, CA, USA) according to the manufacturer's instructions. The enriched protein solutions were reduced with 10 mM dithiothreitol at 56 °C for 1 h. Cysteine residues were blocked with 55 mM iodoacetamide in a dark room for 45 min. Each sample was precipitated with five times the volume of chilled acetone at -20 °C overnight. After centrifugation at 3500 rpm, the pellet was dissolved in 0.5 mM triethyl ammonium bicarbonate and sonicated in ice for 15 min. The total protein concentration was determined using the Bradford method (Solarbio, Beijing, China).

2.5.2. Protein digestion and iTRAQ labeling

Protein solutions (100 μg) of each sample were digested with trypsin and labeled with iTRAQ reagents in accordance with the iTRAQ Reagents Multiplex kit instructions (Applied Biosystems, Foster City, CA, USA). The iTRAQ tags were as follows: 113, Z1; 114, Z2; 116, M1; 117, M2; 118, T1; and 119, T2. The labeled samples were resolved into 20 fractions with an Ultremex SCX column (Phenomenex, USA) containing 5-μm particles (Phenomenex, USA). The eluted fractions were then desalted by Strata X C18 column (Phenomenex, USA) and vacuum dried.

2.5.3. LC-ESI-MS/MS analysis using Q exactive MS

The separated fractions were re-suspended in buffer A (2% acetonitrile, 0.1% formic acid) and centrifuged at 2000 rpm for 10 min. Next, 10-μl aliquots of supernatant were loaded onto a LC-20CE nano HPLC (Shimadzu, Kyoto, Japan). Then, the peptides were transferred onto a C18 column for gradient elution. The samples were loaded at 8 μl/min for 4 min, then the 41-min gradient was run at 300 nl/min starting from 5 to 35% B (98% acetonitrile, 0.1% formic acid), followed by a 5-min linear gradient to 80%, then maintenance at 80% B for 5 min, and finally returning to 5% in 1 min. The obtained peptides were subjected to nanoelectrospray ionization followed by tandem mass spectrometry in a Q Exactive MS (Thermo Fisher Scientific, San Jose, CA) coupled online to the HPLC. Program settings: peptide detection resolution: 70,000; collision energy: 27 V; ion fragment detection resolution: 17,500; electrospray voltage: 1.6 kV; *m/z* scan range for MS: 350–2000 Da; and *m/z* scan range for MS2: 100–1800 Da.

2.5.4. Protein identification and quantitative analysis

For protein identification and quantification, the raw data were converted into MGF format by Proteome Discoverer software 1.2 (Thermo Fisher Scientific, San Jose, CA, USA). The exported MGF files were searched using Mascot search engine (version 2.3.02, Matrix Science, London, UK) against a database including 36,508 sequences (Uniprot *Rattus*, release-2014_12). The search parameters were as follows: enzyme: trypsin; two missed cleavages allowed; taxonomy: *Rattus*; fragment mass tolerance, 0.05 Da; mass values: monoisotopic; variable modifications: oxidation of methionine; peptide mass tolerance: 20 ppm; and fixed modifications: carbamidomethyl of cysteine. In addition, quality control was performed to determine if a reanalysis step was needed. IQuant software (BGI, Shenzhen, China) was applied to the quantification of proteins. The false discovery rate for both protein and peptide identification was set to be less than 0.01. Confident protein identification involved at least two unique peptides. Fold changes > 1.2 or < 0.83 and $p < 0.05$ were set as cut-off values to designate significant protein expression changes.

2.5.5. Pathway and interaction network analysis

Biological function analysis of the identified proteins was performed through the DAVID 6.8 website (https://david.ncifcrf.gov). The Uniprot accession numbers of the identified proteins were changed to relevant gene IDs. The proteins were categorized according to their cellular components, molecular functions, and biological processes. The protein–protein interaction network (PPI) was constructed using the online STRING database (https://string-db.org).

2.5.6. Validation of differentially expressed proteins

An enzyme-linked immunosorbent assay (ELISA) method was used to validate the differentially expressed proteins. The plasma protein level was measured using a commercially available ELISA kit. The assay was prepared according to the manufacturer's instructions. The optical density value was read at 450 nm with a Multiskan GO 1510 ELISA reader (Thermo Fisher Scientific, San Jose, CA, USA).

2.6. Statistical analysis

The experimental results were presented as mean ± SD. Statistical analysis was performed by one-way ANOVA followed by Tukey's multiple comparison test using SPSS software (version 20.0, SPSS, Chicago, IL, USA). Differences with a p-value < 0.05 were considered significant.

3. Results

3.1. Systolic blood pressure changes

As shown in Fig. 1, the systolic blood pressure (SBP) in the model group was significantly elevated compared with that in the normal control group. In the process of administration, the SBP in the model group remained stable and had no significant changes compared with pre-administration. The SBP in the TJT-treated group was significantly lower than that for the model group at the second week ($p < 0.05$). With the prolonging of the administration time, the SBP of the TJT-treated group declined continuously and reached a minimum at the end of the fourth week. These data demonstrated that TJT had an obvious effect on decreasing SBP.

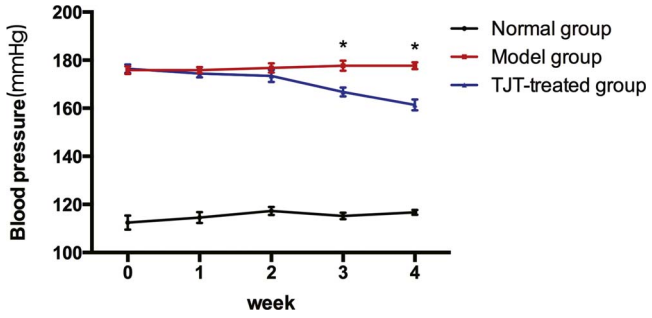

Fig. 1. Effect of oral administration of TJT (100 mg TJT/200g/day for four weeks) on SBP. SBP were recorded in three groups. Data were expressed as mean ± SD (n = 10/group). *$P < .05$ versus the model group.

3.2. Serum metabolite profiling by UPLC-MS

Typical total ion chromatograms of rat serum from the model, TJT-treated, and normal control groups in both positive and negative ion modes are shown in Fig. S1 in the supplementary materials. It was hard to identify the ions that contributed to the discrimination of the TJT-treated and control groups from thousands of signals using traditional statistical methods. PLS-DA is a well-established supervised multivariate statistical analysis method that has been widely used in metabolomic studies. In this study, the PLS-DA method was applied to identify biomarkers that were related to hypertension development.

3.3. Multivariate statistical analysis

PCA and PLS-DA are the two most popular pattern recognition methods used to obtain information for sorting and identifying metabolites. PCA is an unsupervised pattern recognition method for multivariate statistical analysis. The PCA score plots represent a two-dimensional distribution between the model group and the normal group in both positive and negative ion modes (Fig. 2A-1 and B-1). The obvious separation between the model and normal groups suggests that significant serum metabolic disturbance occurred in the SHRs. To further elucidate the differential variables between the two groups, PLS-DA analysis was applied for supervised pattern recognition. Manifested in both positive and negative ion modes, the normal and model groups clustered respectively and separated from each other along the t [1] axis (Fig. 2A-2 and B-2). In the PLS-DA model, the cumulative R2X and Q2 were 0.684 and 0.969, and 0.691 and 0.95, respectively, in different ion modes. No over-fitting was observed according to the results of the permutation test (Fig. 2A-3 and B-3). As shown in Fig. 2A-3 and B-3, the R2Y-intercept was 0.991 and 0.992 in the positive and negative ion modes, respectively. Furthermore, all green R2 values to the left were lower than the original points to the right, indicating that the original model was valid.

3.4. Identification of biomarkers and pathways

To identify biomarkers in the model and normal groups, the variables with VIP values above 1.0 were filtered out. The Student's t-test and fold change were used to reveal the significant differences in the identified metabolites between the model and normal groups. The threshold for statistical significance was set at $p < 0.05$ and $FC > 2$. Potential biomarkers were extracted from the (S)-plot (Fig. 3A-1 and B-1) and the loading plot (Fig. 3A-2 and B-2), which were established based on PLS-DA. The farther a point is away from the center, the more contribution it makes to the difference between the groups and the more likely it is to be a differential metabolite [14]. In the (S)-plot, variables at the bottom left and top right, simultaneously satisfying the conditions of $VIP > 1$, $p < 0.05$, and $FC > 2$, were regarded as potential biomarkers. The selected biomarkers in the loading plot (Fig. 3A-2 and B-2) were in accordance with those in the (S)-plot (Fig. 3A-1 and B-1). The VIP-(S)-plot based on the PLS-DA model was also constructed and is exhibited in Fig. 3A-3 and B-3. Ultimately, under the premise of the above conditions, a total of 23 variables were identified as potential biomarkers and are listed in Table 1. These variables (12 in positive mode, 11 in negative mode) were predicted by comparing the MS and MS/MS fragments with the metabolites found by searching in HMDB, METLIN, and KEGG databases. Seventeen of the 23 biomarkers identified were up-regulated and six of them were depressed in the model group. The related pathways were identified with the MetaboAnalyst tool. The results suggest that these target pathways show marked perturbations in the development of hypertension and could contribute to the development of hypertension. Six main pathological processes, namely linoleic acid metabolism, tryptophan metabolism, glycerol phospholipid metabolism, ether lipid metabolism, sphingolipid metabolism, and arginine and proline metabolism, were involved in hypertension development, indicating that the dysfunctions of multiple pathways were involved in the pathological process of hypertension.

3.5. Metabolomics in TJT intervention

The serum metabolic profiles of the TJT-treated group were obtained by using the UPLC-Q-Exactive-MS method. Based on the preliminary analysis, it is reasonable to take the differential metabolites as the potential drug targets to further investigate the interventional mechanisms of TJT on SHR. Therefore, the levels of the biomarkers were introduced as variables to PCA performed on the normal, model, and TJT-treated groups. The score plot of the PCA showed that the three groups were clearly separated (Fig. 4A and B), and the TJT intervention group was closer to the normal group than the model group. By comparing the identified biomarker levels in the normal, model, and TJT-treated groups, 20 of the identified biomarkers were completely reversed by TJT. Bar graphs of these 20 metabolites in serum with a reversing trend to normal induced by TJT treatment are shown in Fig. 5.

3.6. Differentially expressed proteins

The serum proteome differences between different groups were examined with iTRAQ technology. The relative protein expression values were compared between groups (normal vs. model and TJT vs. model) to identify the differentially expressed proteins (DEPs) that were of great interest for their possible role in disease progression, potential capacity in disease diagnosis, and the revelation of molecular drug targets. The threshold value was set as < 0.83 and > 1.2 fold change and $p < 0.05$. Comparing the 215 proteins identified in the normal vs. model groups with the 39 proteins identified in TJT-treated vs. model groups, there were 14 proteins identified as target proteins of TJT applied to SHR rats. Table 2 shows the proteins identified, including the protein name, gene name, Uniprot accession number, N% coverage, unique peptide, and protein expression ratio. The MS/MS spectra were shown in Fig. S2 in the supplementary materials.

3.7. Bioinformatics analysis

GO enrichment analysis was performed to classify the cellular components, molecular functions, and biological processes that these proteins were involved in, and the results are presented in Fig. 6. The cellular component analysis revealed that most of the DEPs belong to the extracellular exosome, extracellular space, mitochondrion, blood microparticle, extracellular matrix, and mitochondrial outer membrane. They also have distinct molecular functions, mainly involving heparin binding, identical protein binding, peroxidase activity, aldehyde dehydrogenase (NAD) activity, oxygen binding, protease binding, and cysteine-type endopeptidase inhibitor activity. The biological process analysis indicated that these proteins play a role in 17 different biological processes, with majority participating in negative regulation

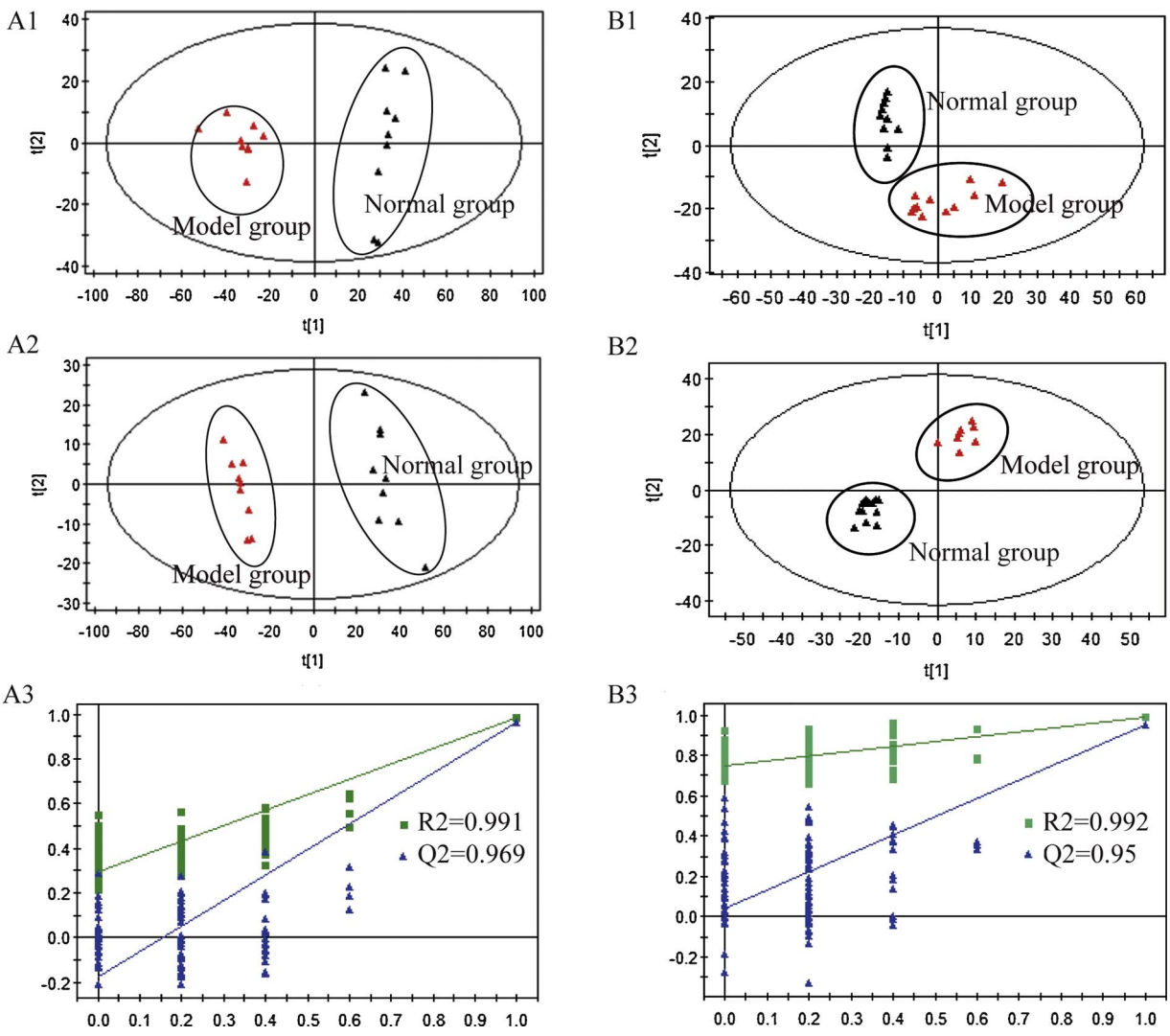

Fig. 2. PCA (A1, B1) and PLS-DA (A2, B2) score plots of rat serum metabolites from the normal group (n = 10) and model group (n = 10) and the permutation tests (A3, B3) for PLS-DA models in positive ion mode (A) and negative ion mode (B). The PCA score plots separated normal group from model group. The PLS-DA score plots indicated a distinct separation between normal group and model group. Validation of the PLS-DA models was randomly permutated for 100 times and the x-axis represents the correlation coefficient between the original y variable and the permutated y variable while the y-axis represents the value of R^2 and Q^2.

of apoptotic processes and response to drugs. From pathway analysis, these proteins were shown to be mainly involved in metabolic pathways, the PPAR signaling pathway, and fatty acid degradation. Additionally, these proteins were also related to beta-alanine metabolism, propanoate metabolism, tryptophan metabolism, and complement and coagulation cascades. The interruption of these pathways may provide a means for the development of molecularly targeted therapies for hypertension. In addition, the PPI networks associated with the DEPs were generated using the STRING database and are shown in Fig. 7.

3.8. Validation of DEPs in serum via ELISA

We then proceeded to quantify the serum levels of MPO and KNG1 using a commercially available ELISA kit to validate their potential as biomarkers. The results demonstrate that the two proteins were significantly elevated or decreased in the serum of the TJT-treated group rats compared with the model rats (Fig. 8), consistent with iTRAQ analysis.

4. Discussion and conclusion

Identifying critical proteins and metabolites as well as the involved pathways that are affected by or respond to a drug in the body using modern technological means is useful to augment our understanding of the interventional mechanisms associated with the drug. Therefore, this study investigated the alterations of protein and metabolic profiles in the serum of rats treated with TJT by using an integrated proteomics and metabolomics approach. Fourteen proteins were found to be differentially expressed in rat serum while 20 metabolites were identified as potential biomarkers.

A previous study performed by Xu et al. [13] identified five key target proteins during TJT treatment in a clinical proteomics test. They found that the level of serum KNG1 was increased after TJT treatment, which was consistent with the results of our study. Moreover, they also discovered that keratin 1 (KRT1) showed an increasing trend after TJT treatment owing to its vital function in the binding of KNG1 to the endothelium. MPO was identified as a target protein in both studies and it could block the kallikrein (KLK) cleavage site on KNG1 through cooperatively binding with KRT1 [15]. In addition, MPO could also impact the PPARγ signaling pathway, as shown in our study and discussed in the following. TJT could regulate the lipid metabolism pathway that will be discussed below, thus influencing the production of nitric oxide synthase (NOS), resulting in the alternation of vascular smooth muscle cells (VSMC) and the appearance of inflammation. Retinol-binding

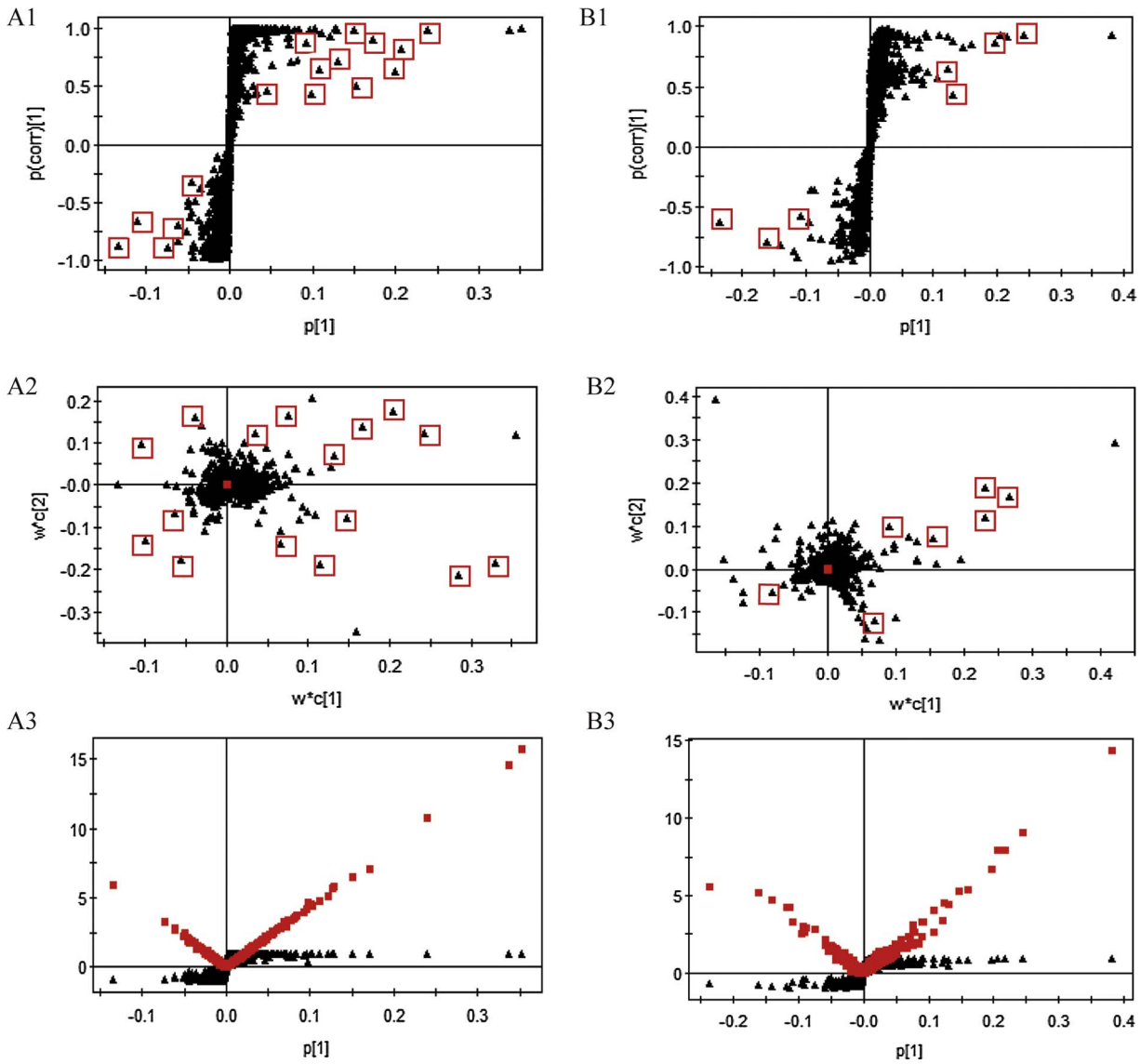

Fig. 3. (S)-plots (A1, B1), loading plots (A2, B2) and VIP-(S)-plots (A3, B3) in PLS-DA analysis of the detected serum metabolites from the normal group (n = 10) and model group (n = 10) rats in positive ion mode (A) and negative ion mode (B). The black triangles represent the retention time and mass data pairs (t_R-m/z) for each metabolite. The red sash represents the potential biomarker.

protein 4 (RBP4) and serum amyloid A protein (SAA), the target proteins discovered by Xu et al. [13], could also damage the NO-dependent vasodilative function through inhibiting the insulin action [16] and causing inflammation, respectively. Fig. 9 shows the interaction network illustrating how TJT exerts its blood pressure reduction effect in the present work.

4.1. Kallikrein–kinin pathway

Composed of KNG, KLK, kininase and kinin, the kallikrein–kinin system (KKS) is an extremely significant and effective blood pressure-regulating system. By indirectly influencing the regulatory function of multiple systems, it has important biological activities. KLK is a group of serine proteases that are present in most tissues and body fluids and is also the major rate-limiting enzyme of the KKS. As a main component of the KKS, KLK plays an essential role in blood pressure regulation and is thus a target for antihypertensive drugs [17]. KNG1 is mainly produced by vascular endothelial cells. It can be specifically cleaved by KLK from the C-terminus to release bradykinin (BK). BK is a major active component of KKS and exerts its actions via G-protein-coupled receptor B1 and B2 subtypes [18,19]. It can stimulate endothelial cells to release endothelial NOS (eNOS) and induce the increased production of nitric oxide (NO) and cyclic guanosine monophosphate (cGMP) through Ca^{2+}-mediated mechanisms, resulting in vasorelaxation [20]. Studies have shown that the content of KNG1 in the urine of patients with pregnancy-induced hypertension is significantly lower than that in normal patients, revealing the inhibited expression of KNG1 in patients with hypertension [21,22]. Kinin is an inflammatory mediator, causing vasorelaxation and increasing vascular permeability. In this study, iTRAQ technology was used to describe the changes in the protein levels in SHRs. The results indicated that TJT could improve the levels of KLKb1 and KNG, ultimately leading to vasorelaxation, which confirmed that TJT was a moderator of KKS.

4.2. Lipid metabolism pathway

As Fig. 9 shows, TJT can change the function of VSMC and affect the production of NO by interfering with lipid metabolic pathways, resulting in vasodilatation. In this study, we found that metabolites such as linoleic acid, phosphatidic acid (PA), lysophosphatidic acid (LPA), LysoPC, 9-OxoODE, 13-OxoODE, 9(S)-HPODE, 12(S)-HPETE, 9,12,13-TriHOME, thromboxane, 5,6-dihydroxyprostaglandin F1α,

Table 1
Identified metabolites showing a difference between the normal and model groups in both positive and negative ion modes. Model group versus normal group: $p < 0.05$, (↑): up-regulated; (↓): down- regulated.

NO.	Name	RT (min)	M/Z	Trend	Elemental composition	Related Pathway
1	Sphinganine	10.64	324.2879	↓	C18H39NO2	Sphingolipid metabolism
2	13-OxoODE	7.01	295.22534	↑	C18H30O3	Linoleic acid metabolism
3	9-OxoODE	7.88	295.2253	↑	C18H30O3	Linoleic acid metabolism
4	Sphinganine 1-phosphate	0	503.30264	↑	C18H40NO5P	Sphingolipid metabolism
5	Thromboxane	14.67	338.3399	↑	C20H32O5	Arachidonic acid metabolism
6	17a-Hydroxypregnenolone	10.17	355.22513	↓	C21H32O3	Steroid hormone biosynthesis
7	Creatinine	3.12	196.12047	↓	C4H7N3O	Arginine and proline metabolism
8	Serotonin	6.39	218.12833	↑	C10H12N2O	Tryptophan metabolism
9	PA(16:0/16:0)	3.32	239.1475	↑	C35H69O8P	Glycerophospholipid metabolism
10	LysoPC (22:4)	4.05	635.3801	↑	C30H54NO7P	Glycerophospholipid metabolism
11	LysoPC (22:5)	3.91	550.33469	↑	C30H52NO7P	Glycerophospholipid metabolism
12	LysoPC (O-18:0)	12.69	554.38098	↑	C26H56NO6P	Glycerophospholipid metabolism
13	L-Arginine	3.31	257.1742	↑	C6H14N4O2	Arginine and proline metabolism
14	9(S)-HPODE	7.87	313.23566	↑	C18H32O4	Linoleic acid metabolism
15	Linoleic acid	3.82	325.21075	↑	C18H32O2	Linoleic acid metabolism
16	LPA (0:0/18:0)	3.26	145.08396	↑	C21H43O7P	Glycerophospholipid metabolism
17	Xanthine	0.89	173.00716	↑	C5H4N4O2	Purine metabolism
18	L-Tryptophan	3.29	407.17153	↓	C11H12N2O2	Tryptophan metabolism
19	9,12,13-TriHOME	6.20	329.23262	↓	C18H34O5	Linoleic acid metabolism
20	Phytosphingosine	6.98	318.2987	↑	C18H39NO3	Sphingolipid metabolism
21	5,6-Dihydroxyprostaglandin F1a	3.64	389.24957	↑	C20H36O7	Arachidonic acid metabolism
22	LysoPC (22:6)	3.97	609.3692	↑	C30H50NO7P	Glycerophospholipid metabolism
23	12(S)-HPETE	6.48	381.22493	↑	C20H32O4	Arachidonic acid metabolism

phytosphingosine, and sphingosine-1P (S1P) increased while sphinganine decreased in the model group, and the level of these metabolites returned to normal after TJT. The above data revealed that lipid metabolism disorders are closely related to hypertension. The antihypertensive effect of TJT may be developed through improving intervention the endothelial function and increasing the NO level, which is consistent with the results of our previous study [23].

Lipid metabolism pathway mainly consists of three parts: glycerophospholipid metabolism, arachidonic acid metabolism, and sphingolipid metabolism. The metabolic changes in serum, including PA, LPA, and LysoPC, were mainly related to glycerophospholipid metabolism. PA can be produced by lecithin under the hydrolysis of phospholipase D, causing calcium mobilization, activating protein kinase C (PKC), and inducing platelet aggregation. PA can then be hydrolyzed by PLA2 to yield LPA. LysoPCs are the main active components of oxidized low-density lipoprotein (Ox-LDL). It is generated by lecithin after being hydrolyzed by PLA2 or lecithin cholesterol acyltransferase formation (LCAT). Previous studies have shown that high metabolic levels of LysoPCs exist in patients with hypertension [24], which is in agreement with the results of our study. LysoPC can lead to an inhibition of vascular endothelial cell proliferation and induce apoptosis, thus creating significant damage to the integrity of the endothelium and affecting its function [25,26]. Once the endothelial cells are damaged, sustained platelet aggregation and the release of active substances will cause thrombosis and smooth muscle cell proliferation [27]. Moreover, studies have shown that LysoPCs can reduce the release of eNOS and inhibit its activity, resulting in endothelium-dependent vasodilative dysfunction [28,29].

The metabolites 9-OxoODE, 13-OxoODE, 9(S)-HPODE, 12(S)-HPETE, 9,12,13-TriHOME, thromboxane, and 5,6-dihydroxyprostaglandin F1α in rat serum including were products of arachidonic acid metabolism. Arachidonate is an unsaturated fatty acid and a precursor of many important eicosanoids. There is increasing evidence that eicosanoids can affect endothelium-dependent vasodilation and play an important role in the incidence of hypertension [30]. Thromboxane (TX) is an end product of arachidonic acid metabolism. TXB2 can elevate blood pressure with its strong effect on promoting thrombocyte aggregation and constricting the blood vessels [31]. In addition, TX and prostaglandin (PG) together participate in the regulation of platelet function and blood vessel tension [32]. TX causes smooth muscle cell proliferation by prohibiting the synthesis of PG and impacting the vascular permeability, thereby increasing the total peripheral resistance to elevate the blood pressure [33].

Past studies have shown that sphingolipid and its metabolites are not only important for making cell membranes, but are also involved in the regulation of cellular proliferation, differentiation, senescence,

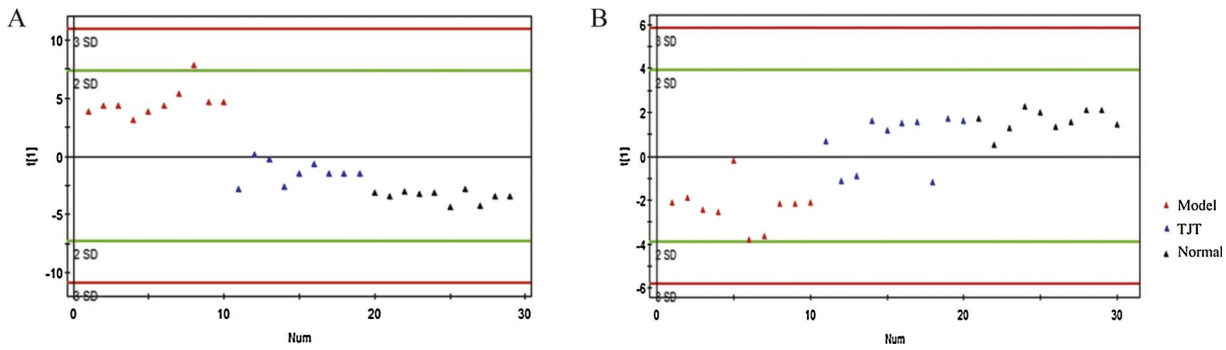

Fig. 4. PCA Score plots from the normal group, model group and TJT-treated group of the reversed metabolites after TJT treatment in positive ion mode (A) and negative ion mode (B). The model group was separated from the normal group obviously and the TJT-treated group was located between the two groups, indicating that the TJT-treated group rats tended to normal.

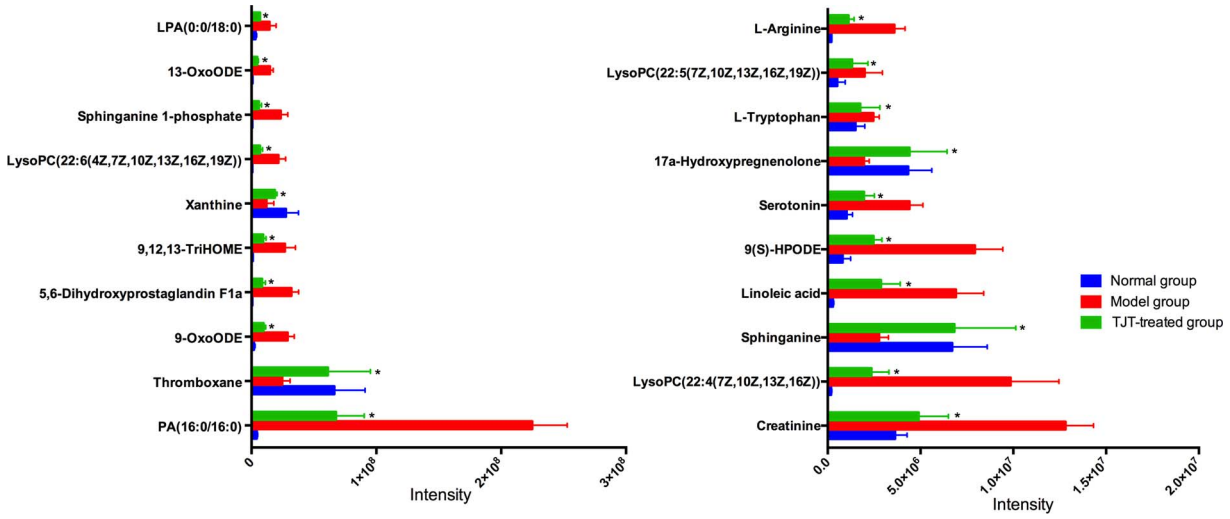

Fig. 5. Bar graph of 20 representative metabolites in serum with a reversing trend to normal induced by TJT treatment. The x-axis indicates the relative peak intensities. Data were expressed as mean ± SD (n = 10/group). $^{*}P < .05$ versus the model group.

apoptosis, and other fundamental signal transduction processes. With the development of the study of the relationship between hypertension and sphingolipid metabolism, it is becoming apparent that sphingosine, ceramide, sphingosine-1-phosphate (S1P), and other intermediate products are associated with hypertension [34]. It is generally known that S1P produced by sphingolipid metabolism can regulate endothelial function by activating NOS or restraining endothelium-derived hyperpolarizing factor (EDHF) [35,36] and inducing the concentration of NO, thereby relaxing blood vessels. In addition, studies have reported that S1P has a vasoconstrictive impact on the coronary arteries, cerebral blood vessels, and other structures [37]. Fenger et al. [38] applied the informationized network analysis method to sphingolipid metabolism and its correlated processes based on a complex network and found that sphingolipid metabolism and its related gene network play an important role in the regulation of blood pressure.

4.3. PPAR signaling pathway

PPAR is a class of ligand-dependent transcription factors, which is widespread in various tissues and organs. It belongs to the intranuclear receptor superfamily, mainly involved in lipid metabolism, inflammatory response, and apoptosis [39]. The superfamily includes three subtypes (α, β, and γ) and the expression of PPARγ changes in a variety of cardiovascular diseases. By affecting the downstream signaling pathways, PPARγ participates in the development of various cardiovascular diseases [40]. Studies have shown that PPARγ is involved in the regulation of blood pressure [41]. PPARγ agonists exhibit antihypertensive effects on hypertensive animal models and can also reduce the incidence of hypertensive complications [42–45]. In this study, TJT was able to act on the PPAR signaling pathway, thus influencing the expression of PPARγ. The variation of PPARγ adversely affected the expression of long chain fatty acid CoA ligase 1 (Acls1), peroxisomal bifunctioanl enzyme (Ehhadh), and Glycerol kinase (GK) through protein–protein interactions and participated in the regulation of blood pressure by affecting the lipid metabolism pathway altering the expression of the above three substances. In addition, the expression level of Ehhadh could be affected by MPO, aldehyde dehydrogenase (Aldh2), and methylmalonate-semialdchyde dehydrogenase (Alda6a1), which were also identified in our study.

PPI network analysis can help in understanding the molecular mechanisms of various diseases from a systemic perspective and discover new drug targets. In this study, the PPI network of the differential proteins was built with the online STRING database. As shown in Fig. 7, the circles represent proteins while the straight lines represent the interactions between different proteins. The line color indicates the type of interaction evidence. Through the construction of interaction networks between proteins, we can generally understand the relevance of different proteins, thus providing evidence for analyzing the relationship between proteins and metabolites. As illustrated in Fig. 9, some proteins, including MPO, Aldh2, and Alda6a1, can influence the

Table 2
The proteins identified as differentially expressed with iTRAQ-based proteomics technology.

No.	Uniprot accession	Gene ID	Protein name	Gene name	Coverage (%)	Unique peptide	MW (kDa)	Ratio(M/T)	P-value
1	Q5FVS2	25048	Kallikrein B, plasma 1	Klkb1	23.8	14	73.33	0.61	0.002
2	A0A0G2K1A2	303413	Protein Mpo	Mpo	13.6	11	59.87	1.82	0.025
3	Q5PQU1	24903	Kininogen 1	Kng1	16	2	48.8	0.66	0.001
4	D3ZCI0	79223	Glycerol kinase	Gk	11.8	6	58.21	1.51	0.018
5	P07896	171142	Peroxisomal bifunctional enzyme	Ehhadh	3.2	3	79.16	1.53	0.035
6	F1LN88	29539	Aldehyde dehydrogenase, mitochondrial	Aldh2	23.7	10	56.98	1.64	0.017
7	Q02253	81708	Methylmalonate-semialdehyde dehydrogenase [acylating], mitochondrial	Aldh6a1	5.8	3	58.21	1.75	0.011
8	P18163	25288	Long-chain-fatty-acid–CoA ligase 1	Acsl1	4.9	3	79.14	1.88	0.001
9	Q5M8C3	246328	Protein Serpina4	SerPina4	42.8	15	48.1	1.83	0.002
10	P02770	24186	Serum albumin	Alb	72	39	70.7	0.39	0.000
11	F1LST1	25661	Fibronectin	Fn1	42.4	11	203.8	1.73	0.035
12	Q71SA3	445442	Thrombospondin 1	Thbs1	52.9	52	133.6	1.69	0.000
13	P01946	25632	Hemoglobin alpha	Hba1	57.7	6	15.5	1.5	0.007
14	P24090	25373	Alpha-2-HS-glycoprotein	Ahsg	35.5	10	38.7	1.79	0.003

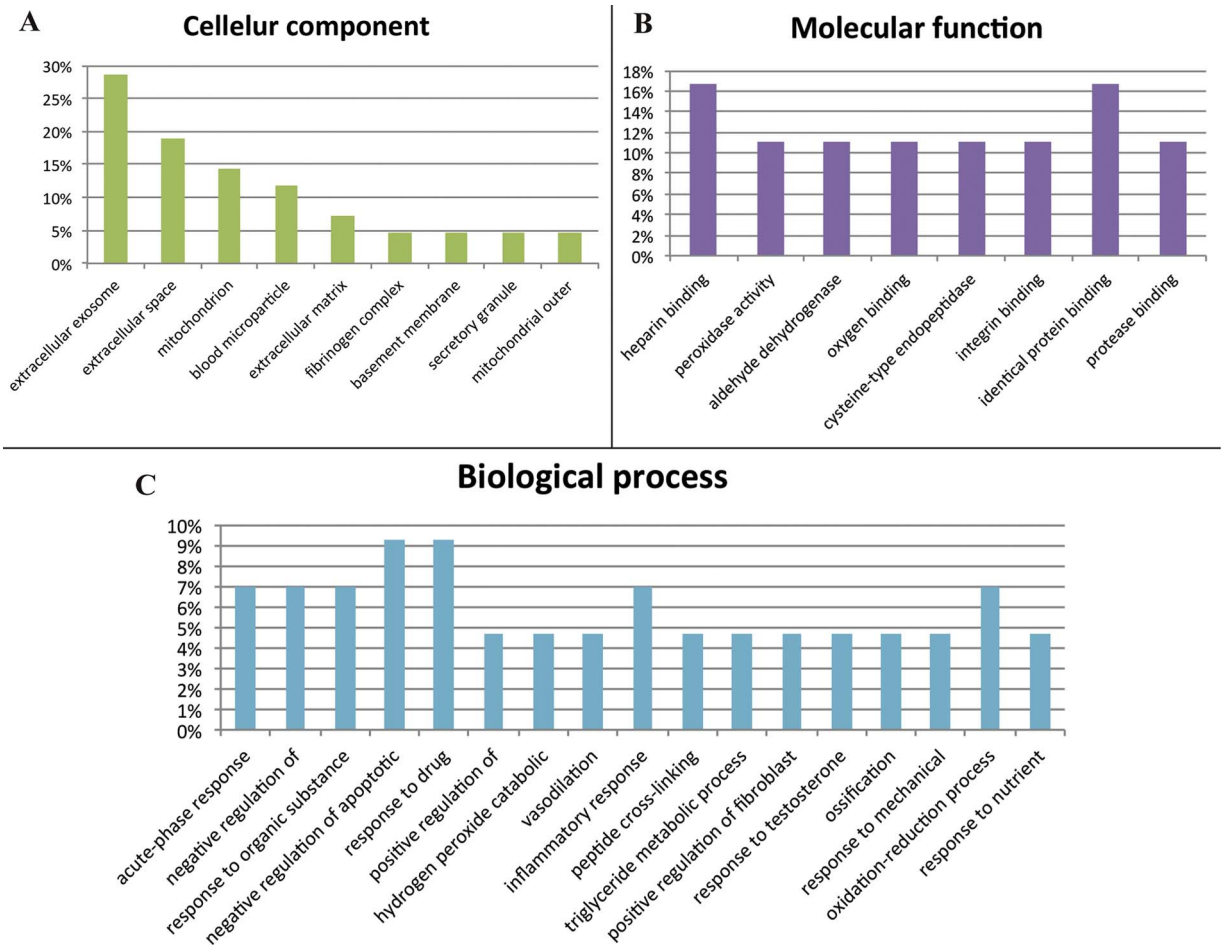

Fig. 6. The proportion of the differentially expressed proteins categorized by function. A: Gene Ontology analysis for cellular components; B: Gene Ontology analysis for molecular function; C: Gene Ontology analysis for biological processes.

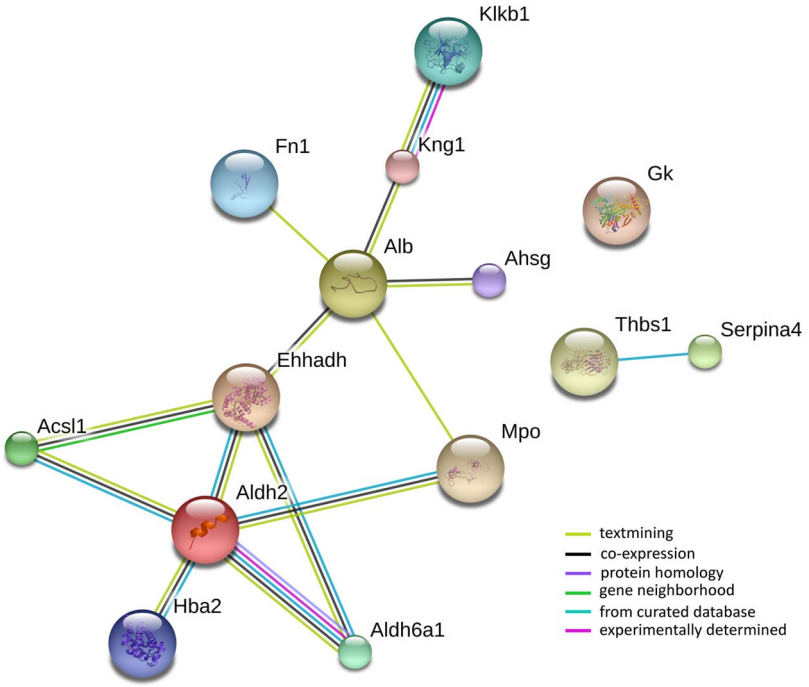

Fig. 7. Protein-protein interaction networks analysis of the differentially expressed proteins with the STRING. The circles represent proteins while the straight lines represent the interactions between different proteins. The color of the edges indicates the type of evidence for the connection.

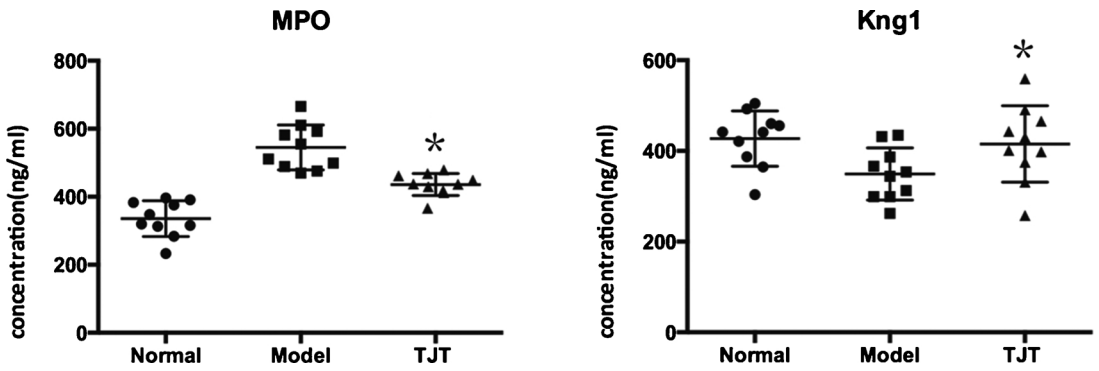

Fig. 8. Validation of the differentially expressed proteins in rat serum by ELISA. The levels of MPO and Kng1 in rat serum were determined with ELISA kits according to the protocol, respectively. Compared with the model group, the TJT-treated group showed a declining trend in the level of MPO and a rising trend in the level of Kng1. Data were expressed as mean ± SD (n = 10/group). $^{*}P < .05$ versus the model group.

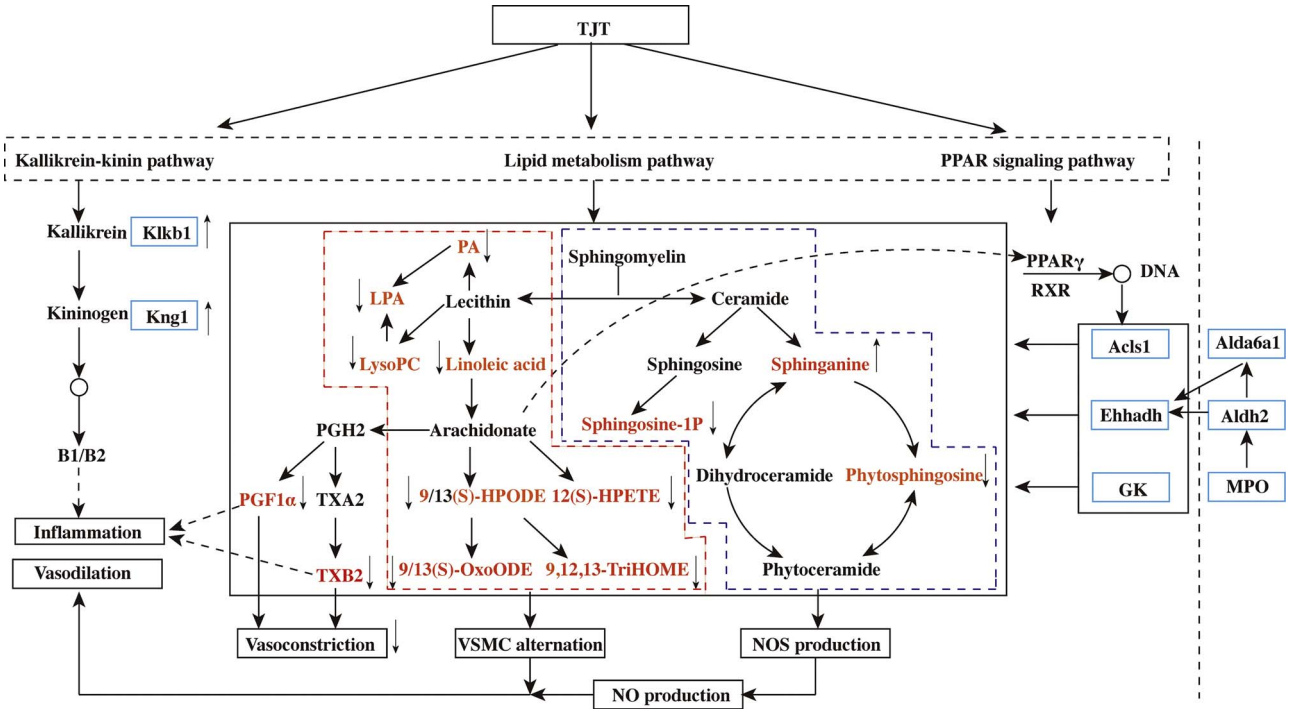

Fig. 9. The perturbed metabolites, proteins and corresponding metabolic pathways related to TJT treatment by integrating the proteome and metabolome data sets. Elevation (up thin arrows) and reduction (down thin arrows) of the levels of metabolites and proteins observed in rat serum were indicated. The metabolites were presented with orange texts and the proteins were circled by blue box.

expression of Ehhadh, which can act on the lipid metabolism pathway together with Acls1 and GK. Although the combination of proteomics and metabolomics was a useful method in this study, there are still some limitations in the method itself. It supposes that a correlation exists between the changes in protein abundance and metabolite concentration. In fact, there are complex regulatory relationships between most enzymes and metabolites and they may not necessarily follow similar trends. Thus, some important information that suggests a link between proteins and metabolites may be overlooked. In addition, there is a dire need for efficient and free software for integrating proteomics and metabolomics.

4.4. Conclusion

The combination of proteomic and metabolomic techniques developed for evaluating the therapeutic effect and mechanism of action of TJT on hypertension was found to be reliable in our study. The complete analysis indicated that TJT could exert its therapeutic effect through three biological pathways: the kallikrein–kinin pathway, the lipid metabolism pathway, and the PPARγ signaling pathway. Combinations of metabolomics and proteomics data can be employed in our future work.

Disclosure of interest

The authors declare that they have no conflicts of interest concerning this article.

Acknowledgments

The work was supported by National Natural Science Foundation and Postdoctoral Science Foundation of China (No. 81273700, NO. 2014M551952).

Appendix A. Supplementary data

Supplementary material related to this article can be found, in the online version, at doi:https://doi.org/10.1016/j.biopha.2018.02.025.

References

[1] S. Gioria, J. Lobo Vicente, P. Barboro, R. La Spina, G. Tomasi, P. Urbán, A. Kinsner-Ovaskainen, R. François, H. Chassaigne, A combined proteomics and metabolomics approach to assess the effects of gold nanoparticles in vitro, Nanotoxicology 10 (2016) 736–748.

[2] B.S. Dos Santos, L.C. da Silva, T.D. da Silva, J.F. Rodrigues, M.A. Grisotto, M.T. Correia, T.H. Napoleão, M.V. da Silva, P.M. Paiva, Application of omics technologies for evaluation of antibacterial mechanisms of action of plant-derived products, Front. Microbiol. 7 (2016) 1466.

[3] W.H. Heijne, A.S. Kienhuis, B. van Ommen, R.H. Stierum, J.P. Groten, Systems toxicology: applications of toxicogenomics, transcriptomics, proteomics and metabolomics in toxicology, Expert. Rev. Proteom. 2 (2005) 767–780.

[4] K.F. Zhang, X.D. Pan, J. Zheng, D. Xu, J. Zhang, L.Z. Sun, Comparative tissue proteomics analysis of thoracic aortic dissection with hypertension using the iTRAQ technique, Eur. J. Cardiothorac. Surg. 47 (2015) 431–438.

[5] A.Y. Hwang, C. Dave, S.M. Smith, Trends in antihypertensive medication use among US patients with resistant hypertension, 2008 to 2014, Hypertension 68 (2016) 1349–1354.

[6] P.M. Kearney, M. Whelton, K. Reynolds, P. Muntner, P.K. Whelton, J. He, Global burden of hypertension: analysis of worldwide data, Lancet 365 (2005) 217–223.

[7] S.S. Yoon, Q. Gu, T. Nwankwo, J.D. Wright, Y. Hong, V. Burt, Trends in blood pressure among adults with hypertension: United States, 2003 to 2012, Hypertension 65 (2015) 54–61.

[8] J.A. Whitworth, World Health Organization, International Society of Hypertension Writing Group, World Health Organization (WHO)/International Society of Hypertension (ISH) statement on management of hypertension, J. Hypertens. 21 (2003) (2003) 1983–1992.

[9] C. Bavishi, S. Bangalore, F.H. Messerli, Renin angiotensin aldosterone system inhibitors in hypertension: is there evidence for benefit independent of blood pressure reduction, Prog. Cardiovasc. Dis. 59 (2016) 253–261.

[10] A.C. Cameron, N.N. Lang, R.M. Touyz, Drug treatment of hypertension: focus on vascular health, Drugs 76 (2016) 1529–1550.

[11] X.K. Zhao, Y.D. Li, M.X. Feng, K. Liu, K.B. Chen, Y.Q. Lu, S.B. Sun, P. Song, Chinese herbal medicine for the treatment of primary hypertension: a methodology overview of systematic reviews, Syst. Rev. 5 (2016) 180.

[12] H.Q. Jiang, Z.Z. Shen, Y.J. Chu, Y.L. Li, J.H. Li, X.M. Wang, W.Q. Yang, X.Y. Zhang, J.Q. Ju, J.W. Xu, C.H. Yang, Serum metabolomics research of the anti-hypertensive effects of Tengfu Jiangya tablet on spontaneously hypertensive rats, J. Chromatogr. B: Anal. Technol. Biomed. Life Sci. 1002 (2015) 210–217.

[13] J.W. Xu, Y.L. Li, S.J. Zhang, H.Q. Jiang, N. Wang, H.Q. Lin, Identification of Tengfu Jiangya tablet target biomarkers with quantitative proteomic technique, Evid. Based. Complement. Altern. Med. 2017 (2017) 7594805.

[14] X.L. Zhong, Y.M. Zhong, K.Q. Yan, X.R. Xiao, L. Duan, R.L. Wang, L.Y. Wang, Metabolomics approach based on UHPLC–Q-TOF-MS to identify the chemical constituents of the traditional Chinese Er-Zhi-Pill, J. Sep. Sci. 40 (2017) 2713–2721.

[15] J.M. Astern, W.F. Pendergraft 3rd, R.J. Falk, J.C. Pendergraft, A.H. Schmaier, F. Mahdi, G.A. Preston, Myeloperoxidase interacts with endothelial cell-surface cytokeratin 1 and modulates bradykinin production by the plasma Kallikrein-Kinin system, Am. J. Pathol. 171 (2007) 349–360.

[16] K.M. Farjo, R.A. Farjo, H. Stacey, M. Gennadiy, X.M. Jian, Retinol-binding protein 4 induces inflammation in human endothelial cells by an NADPH oxidase- and nuclear factor kappa B-dependent and retinol-independent mechanism, Mol. Cell. Biol. 32 (2012) 5103–5115.

[17] L. Waeckel, L. Potier, C. Chollet, C. Taveau, P. Bruneval, R. Roussel, F. Alhenc-Gelas, N. Boub, Antihypertensive role of tissue kallikrein in hyperaldosteronism in the mouse, Endocrinology 153 (2012) 3886–3896.

[18] Y.D. Fukuhara, R. Dellalibera-Joviliano, F.Q. Cunha, M.L. Reis, E.A. Donadi, The kinin system in the envenomation caused by the Tityus serrulatus scorpion sting, Toxicol. Appl. Pharmacol. 196 (2004) 390–395.

[19] A.R. Meki, H.E. Omar, A bradykinin-potentiating fraction isolated from the venom of Egyptian scorpion Buthus occitanus induced prostaglandin biosynthesis in female guinea pigs, Comp. Biochem. Physiol. C: Pharmacol. Toxicol. 116 (1997) 183–189.

[20] P.M. Vanhoutte, C.M. Boulanger, J.V. Mombouli, Endothelium-derived relaxing factors and converting enzyme inhibition, Am. J. Cardiol. 76 (1995) 3E–12E.

[21] J.Y. Hu, H.X. Guo, S.W. Hu, C.H. Wang, Urine proteome analysis of gestational hypertension and healthy pregnant women, J. Pract. Obstet. Gynecol. 29 (2013) 446–449.

[22] H.X. Guo, J.Y. Hu, S.W. Hu, C.H. Wang, J. Wang, Content change of kininogen-1 in urine of patients with gestational hypertension, Matern. Child. Health China 15 (2015) 2339–2341.

[23] H.Q. Jiang, Z.Z. Shen, Y.J. Chu, Y.L. Li, J.H. Li, X.M. Wang, W.Q. Yang, X.Y. Zhang, J.Q. Ju, J.W. Xu, C.H. Yang, Serum metabolomics research of the anti-hypertensive effects of Tengfu Jiangya tablet on spontaneously hypertensive rats, J. Chromatogr. B: Anal. Technol. Biomed. Life Sci. 1002 (2015) 210–217.

[24] H.Q. Jiang, Y.L. Li, J. Xie, Serum metabonomics analysis of hypertension based on HPLC-ESI-TOF-MS, J. Shandong Univ. Health Sci. 49 (2011) 150–159.

[25] M. Takahashi, H. Okazaki, Y. Ogata, K. Takeuchi, U. Ikeda, K. Shimada, Lysophosphatidylcholine induces apoptosis in human endothelial cells through a p38-mitogen-activated protein kinase-dependent mechanism, Atherosclerosis 49 (2002) 387–394.

[26] Y. Rikitake, S. Kawashima, T. Yamashita, T. Ueyama, S. Ishido, H. Hotta, K. Hirata, M. Yokoyama, Lysophosphatidylcholine inhibits endothelial cell migration and proliferation via inhibition of the extracellular signal-regulated kinase pathway, Arterioscler. Thromb. Vasc. Biol. 20 (2000) 1006–1012.

[27] N. Kume, M.J. Gimbrone, Lysophosphatidylcholine transcriptionally induces growth factor gene expression in cultured human endothelial cells, J. Clin. Invest. 93 (1994) 907–911.

[28] E. Millanvoye-Van Brussel, G. Topal, A. Brunet, T. Do Pham, V. Deckert, F. Rendu, M. David-Dufilho, Lysophosphatidylcholine and 7-oxocholesterol modulate Ca2+ signals and inhibit the phosphorylation of endothelial NO synthase and cytosolic phospholipase A2, Biochem. J. 380 (2004) 533–539.

[29] R.K. Davda, K.T. Stepniakowski, G. Lu, M.E. Ullian, T.L. Goodfriend, B.M. Egan, Oleic acid inhibits endothelial nitric oxide synthase by a protein kinase C-independent mechanism, Hypertension 26 (1995) 764–770.

[30] N. Li, J.Y. Liu, H. Qiu, T.R. Harris, P. Sirish, B.D. Hammock, N. Chiamvimonvat, Use of metabolomic profiling in the study of arachidonic acid metabolism in cardiovascular disease, Congest Heart Fail. 17 (2011) 42–46.

[31] L.C. Pettigrew, J.C. Grotta, H.M. Rhoades, K.K. Wu, Effect of thromboxane synthase inhibition on eicosanoid levels and blood flow in ischemic rat brain, Stroke 20 (1989) 627–632.

[32] X. De Leval, J. Hanson, J.L. David, B. Masereel, B. Pirotte, J.M. Dogné, New developments on thromboxane and prostacyclin modulators part II: prostacyclin modulators, Curr. Med. Chem. 11 (2004) 1243–1252.

[33] I.A. Jagroop, I. Clatworthy, J. Lewin, D.P. Mikhailidis, Shape change in human platelets: measurement with a channelyzer and visualization by electron microscopy, Platelets 11 (2000) 28–32.

[34] L.J. Spijkers, R.F. van den Akker, B.J. Janssen, J.J. Debets, J.G. De Mey, E.S. Stroes, B.J. van den Born, D.S. Wijesinghe, C.E. Chalfant, L. MacAleese, G.B. Eijkel, R.M. Heeren, A.E. Alewijnse, S.L. Peters, Hypertension is associated with marked alterations in sphingolipid biology: a potential role for ceramide, PLoS One (6) (2011) e21817.

[35] A.C. Mulders, M.C. Hendriks-Balk, M.J. Mathy, M.C. Michel, A.E. Alewijnse, S.L. Peters, Sphingosine kinase-dependent activation of endothelial nitric oxide synthase by angiotensin II, arterioscler, Thromb. Vasc. Biol. 26 (2006) 2043–2048.

[36] A.C. Mulders, M.J. Mathy, D. Meyer zu Heringdorf, M. ter Braak, N. Hajji, D.C. Olthof, M.C. Michel, A.E. Alewijnse, S.L. Peters, Activation of sphingosine kinase by muscarinic receptors enhances NO-mediated and attenuates EDHF-mediated vasorelaxation, Basic Res. Cardiol. 104 (2009) 50–59.

[37] D.G. Hemmings, Signal transduction underlying the vascular effects of sphingosine 1-phosphate and sphingosylphosphorylcholine, Naunyn Schmiedebergs Arch. Pharmacol. 373 (2006) 18–29.

[38] M. Fenger, A. Linneberg, J. Jeppesen, Network-based analysis of the sphingolipid metabolism in hypertension, Front. Genet. 6 (2015) 84.

[39] X.Y. Zhao, J.L. Su, Advances in cardiovascular protection of PPARα, PPARγ and its agonists, Chongqing Med. J. 19 (2010) 2680–2682.

[40] J.J. Ma, T. Zhang, Advances in research on the relationship between PPARγ and disease, Chin. Pharmacol. Bull. 28 (2012) 601–604.

[41] T. Roszer, M. Ricote, PPARs in the renal regulation of systemic blood pressure, PPAR Res. 2010 (2010) 1–12.

[42] A. Sakamoto, M. Hongo, K. Saito, R. Nagai, N. Ishizaka, Reduction of renal lipid content and proteinuria by a PPAR-γagonist in a rat model of angiotensin II-induced hypertension, Eur J. Pharmacol. 682 (2012) 131–136.

[43] S.H. Chan, K.L. Wu, P.S. Kung, J.Y. Chan, Oral intake of rosiglitazone promotes a central antihypertensive effect via up-regulation of peroxisome proliferator-activated receptor-gamma and aleviation of oxidative stress in rostral ventrolateral medula of spontaneously hypertensive rats, Hypertension 55 (2010) 1444–1453.

[44] R. Hernanz, A. Martíná, J.V. Pérez-Girón, R. Palacios, A.M. Briones, M. Miguel, M. Salaices, M.J. Alonso, Pioglitazone treatment increases COX-2-derived prostacyclin production and reduces oxidative stress in hypertensive rats: roles in vascular function, Br. J. Pharmacol. 16 (2012) 1303–1319.

[45] A. Sugawara, A. Uruno, M. Kudo, M. Kudo, K. Matsuda, C.W. Yang, S. Ito, Effects of PPARγ on hypertension, atherosclerosis, and chronic kidney disease, Endocr. J. 57 (2010) 847–852.